Analyses of size distribution and related lung deposition in the *SELSONICS* Ultrasonic Nebulization Chamber

P. Madl & W. Hofmann

Department of Materials Engineering & Physics – Division of Physics and Biophysics
- Working Group of Radiation and Environmental Biophysics,
University of Salzburg, A-5020 Salzburg, Austria

Universität Salzburg

Department of Materials Engineering & Physics – Division of Physics and Biophysics
Radiation and Environmental Biophysics Working Group

Abstract

Vitamin-C enriched sodium-chloride (15% NaCl solution) from the Dead Sea and organically grown and extracted olive-oil samples with traces of supplemented Vitamin-D (totalling 5mL each) were separately nebulized by ultrasound atomizers in a therapeutic aerosol chamber constructed by Selsonics GmbH. Particle growth dynamics from aerosol processing reactions were measured with a Scanning Mobility Particle Sizer (SMPS) immediately after a 3 minutes long sample injection sequence. Scanning times with the SMPS covered a potential exposure window of at least 9 minutes in the size range of 0.01 to 1.1 µm. Based on the data obtained from the SMPS measurements, the stochastic lung particle deposition model IDEAL-2 (Koblinger & Hofmann, 1990; Hofmann & Koblinger, 1990) was applied and the associated particle deposition analyzed.

Introduction

Aerosol inhalation using Selsonic's exposure chamber is achieved via two separate ultrasound nebulizers. Two vials containing 5mL each - one filled with vitamin-C enriched saltwater from the Dead Sea, the other with vitamin-D enriched olive oil - are placed into separate drawers (see Fig. 1). Once the vials are in place, an automated procedure operates the nebulization routine, starting with a 5 minute long salt-exposure (of which 3 minutes constitute the actual nebulization window), followed by an identical sequence in which the oil is vaporized. In-between the samples as well as at the end and of the exposure, the chamber is flushed via two powerful ventilation fans.

Fig. 1: Selsonic's nebulization chamber. The nebulizer on the top left (1) is used to emit the NaCl aerosol, whereas the one on the top right (2) is used for olive-oil vaporization. The drawers for the vials (3) house the monousable NaCl- and oil vials respectively (image: Selsonics, 2007).

Methods

Nebulization of both 5mL liquid salt and oil samples was carried out by atomizers using ultrasound technology. Measurements of the nebulized samples were made with the SMPS model (Grimm Aerosol Technik). This mobile continuous nano-particle counter combines a Condensation Nucleus Counter (model #5.403) and a Direct Mobility Analyzer „Vienna-Type", (model #5.500), using a L-DMA suitable to detect a size range between 10 to 1100 nm.
The observed particle spectra of the oil- and NaCl-samples are documented in Fig. 2. It reveals a polydisperse distribution with the geometric mean located at around 140 nm. Particle concentrations peaked at around $103 \cdot 10^3 \pm 26 \cdot 10^3$ particles·cm^{-3} and gradually decreased afterwards as agglomeration to larger clusters took place. In the same figure, the observed particle spectrum of the NaCl-sample is incorporated. Here, the geometric mean was located at around 240 nm, while particle concentrations peaked at around $30 \cdot 10^3 \pm 4.8 \cdot 10^3$ particles·cm^{-3} and gradually decreased afterwards due to agglomeration to larger clusters.

To investigate the fate of inhaled particles, we applied the stochastic lung model developed by Koblinger and Hofmann (1990a,b) to model deposition over the size range of 10 to 1100 nm using the 44 output channels of the SMPS – each channel corresponds to a specific size class with a corresponding number particle concentration. The pairs of number concentration and size class were used to run the stochastic model. In this model the geometry of the airways along the path of an inhaled particle is selected randomly using a Monte Carlo code IDEAL-2, whereas deposition probabilities are computed by deterministic formulae. In addition, the airway geometry selection, the random walk of particles through this geometry and the methods of aerosol deposition calculation in conductive and respiratory airways during a full breathing cycle are incorporated in this model. Altogether, the model enables computation of total, regional and differential particle deposition in a stochastic lung structure.

Figures 3.a,b reveal the potential deposition patterns of the samples within the human lung. The frequency on the left ordinate is plotted as a dimensionless parameter, thus given in percent when multiplied by a conversion factor of 100. The right ordinate refers to the same set of data and presents the absolute number particle concentrations with respect to each generation. Generation-numbers plotted on the abscissa correspond to the various pulmonary regions, with the trachea being generation 0, while generation 1 to 15 are associated to the bronchial region. The regimes above are related to the alveolar regime (Yeh & Schum, 1980). It was assumed that particle morphology corresponds to a spherical shape with a particle density of ρ=1g/cm^3.

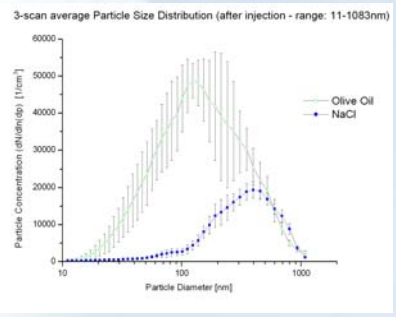

Fig. 2: Size class particle distribution of an olive-oil- and NaCl aerosol over a time window of 9 minutes. Average total particle concentration of olive oil was found at $103 \cdot 10^3 \pm 26 \cdot 10^3$ cm^{-3} and that of NaCl at $30 \cdot 10^3 \pm 4.8 \cdot 10^3$ cm^{-3}.

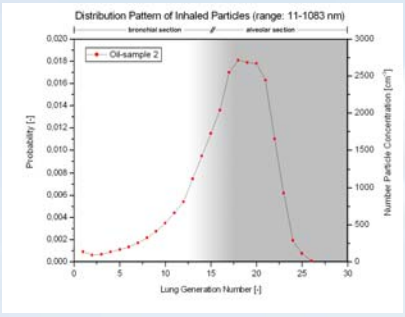

Fig. 3a: Modelled distribution of the olive-oil aerosol deposition within the respiratory tract over 27 generations. Extrathoracic deposition 8.93% - total lung deposition: 25.8%.

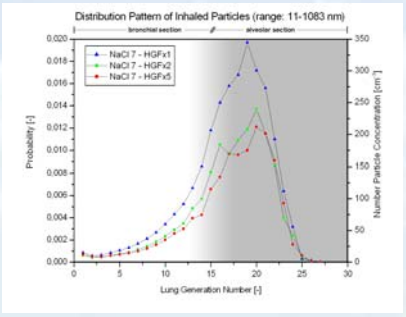

Fig. 3b: Modelled distribution of NaCl-aerosol deposition within the respiratory tract.
HGFx1: extrathoracic deposition: 10.0% - total lung deposition: 29.9%.
HGFx2: extrathoracic deposition: 7.92% - total lung deposition: 20.9%.
HGFx5: extrathoracic deposition: 6.14% - total lung deposition: 16.2%.

Results

Particle deposition of the nebulized oil sample outlines the deep-reaching pulmonary properties of this aerosol. Due to the minute size of the particle load along with the hydrophobic attribute of this sample, bronchial deposition is negligible. Particle deposition of the nebulized NaCl sample follows a similar distribution pattern. However, a proportionally larger fraction is deposited within the tracheo-bronchial regime. With relative humidity levels in the human respiratory tract equalling almost 100%, the hydrophilic character of this sample results in additional deposition within the bronchial regime.

Conclusion

Using nano-sized particles greatly enhances the penetration efficiency to evoke various responses of the human body. As observed in Fig. 3 a-b, the size range of the inhaled particles easily reaches the alveolar region well beyond the 15th lung generation. Alveolar congestion by the inhaled particle load can largely be excluded, as the detected nano-particles are some $1 \cdot 10^3$ to $10 \cdot 10^3$ times smaller than the tiniest alveolar duct-diameters (Burri, 1985). As shown in Fig. 2, the potentially huge bolus concentration of the olive oil spectrum, amounting to approx. $103 \cdot 10^3$ particles·cm^{-3} is spread over 27 lung generations further dividing the overall concentration by an approximated factor of 2^{27}. Considering particle kinetics after aerosol injection within the chamber along with the volume of air to be inhaled, one can expect a slightly elevated inhaled particle load as the SMPS sampled the chamber by a continuous flow of 0.3 L/min only. That is, a relaxed person inside the chamber would have a tidal respiratory volume of about 0.5 L along with roughly 12 in-/exhalations per minute, which yields a total of 6 L of inhaled respiratory air. In relation to the 0.3 L/min of the sampling device, this corresponds to a 20-fold increase of the inhaled particle load. Since total scanning windows of the SMPS lasted 9 minutes for each nebulized sample and the fact that a person would just be exposed to 5 minutes per sample each – with flushing cycles in-between – the actual proportionality factor would just be 5/9th of 20 – or roughly 11-times the detected SMPS-concentrations. Figures 3 a-b clearly highlight the partial deposition efficiency modeled with the measured data. In the case of olive oil inhalation about 26% and in the case of sodium chloride between about 16% are deposited within the entire respiratory tract – which includes the extrathoracic deposition.
Nebulization of hydrophilic and hydrophobic substances is not only limited to inhalation per se, whole body dermal exposure is another issue to consider. Dermal and inhalatory absorption of nano-sized aerosols can be considered as being ideal size classes for rapid phagocytic and selective uptake by the exposed cells (Mulz, 2007).

Since there is no sharp threshold between these two regions in a realistic lung structure, for simplicity Yeh and Schum (1980) separated these two regions by assigning those above the 15th generation alveolar status whereas those below belong to the bronchial region.
Based on these assumptions hydrophobic particles such as nebulized olive oil tend to increasingly deposit in higher generation airways (alveolar regime), and to a lesser extent into within the bronchial region where ciliary motion would translocate deposited particles promptly via the mucociliary clearance. Hence, alveolar deposition is associated with an increased imuno-response activity by alveolar macrophages (Donaldson et al., 1998).

It has been demonstrated that sniffing nano-sized aerosols not only easily pass the blood-brain barrier via humoral transport, but they are also readily absorbed via skin and mucous membranes (Buchbauer, 2003). Both percutane absorption and inhalation of nano-sized aerosols get rid of the so-called first-pass effect (FPE) – that is the biological transformation and, in some cases, elimination of a substance in the liver after absorption from the intestine and before it reaches systemic circulation (Gold & Sehmi, 2004). Elimination of the FPE would enable exposure to considerably lower dosage of the substances involved and as a result could significantly reduce potential side effects.
As outlined by the potential application in treating respiratory ailments from people experiencing increased respiratory airflow resistance (Daviskas et al., 1996), Franca Angerosa (1995) highlighted the aroma-therapeutic aspect of virgin olive oil inhalation to stimulate the proteic receptors and neurons of the olfactory system. Moreover, the vast number of C_6-volatiles, aldehydes, alcohols and esters are directly routed into the cells without being subject to the FPE. Goldfrank et al. (2002) emphasized the decontaminant properties of olive oils in dermal application, as it absorbs toxic substances like phenols and prevent their further absorption. In addition, the authors state that cutaneous decontamination decreased systemic effects and facilitated healing of dermal burns. Hence it may not come as a surprise that whole-body aerosol exposure of other ethereal oils and/or watery solutions along with aerosol inhalation may proof far more efficient than conventional inhalation therapy using a mouth-piece only. This chamber could evoke interest rehabilitation and reconstituting applications, but also in medical studies investigating therapeutical effects in the treatment of *Actelectasis*, hay-fever, neurodermitis (*Atopic dermatitis*), psoriasis, etc. and even in post-scar treatment smoothening hardened dermal scar-tissue (Mulz, 2007). The 5mL required could prove sufficient to achieve respiratory relief in people with cardiovascular and respiratory difficulties (Daviskas et al., 1996; Mulz, 2007).

Acknowledgements

The authors wish to thank to the people from Selsonics for their kind assistance, in particular to *P.Huber* technical officer at Selsonics and to Mr. *P.Richter*, managing director of Selsonics GmbH.
URL: http://www.selsonics.com/Selsonics_E/produkt_e.html

References

Angerosa F., 1995. Sensory Qualities of olive Oils; in the Handbook of Olive Oil: Analysis and Properties; by Harwood J.L., Aparicio R., Harwood J. (eds.), Springer Verlag, p. 360.
Buchbauer G., 2003. Biologische Wirkungen von Ätherischen Ölen und Duftstoffen; 2003. Plenarvortrag am 33. Internationalen Symposiums über Ätherische Öle (ISEO) in Lissabon, ÖAZ 14/2003 p. 76
Burri P.H., 1985. Morphology and Respiratory Function of the Alveolar Unit. International Archives of Allergy and Applied Immunology, no. 76.
Daviskas E, Anderson SD, Gonda I, Eberl S, Meikle S, Seale JP, Bautovich G. 1996. Inhalation of hypertonic saline aerosol enhances mucociliary clearance in asthmatic and healthy subjects; European Respiratory Journal; 9, pp. 725–73
Donaldson K. Li X.Y. MacNee W. 1998. Ultrafine (Nanometre) Particle Mediated Lung Injury. Journal of Aerosol Science, Volume 29, Issues 5-6
Gold V., Sehmi P., 2004. Compendium of Chemical Terminology. International Union of Pure and Applied Chemistry (IUPAC), 76, p. 1052.
Goldfrank L.R., Flomenbaum N., Lewin N., Howland M.A., Hoffman R., Nelson L., 2002. Antiseptics, Desinfectants and Sterilants; in Goldfrank's Toxicologic Emergencies, 7th ed., Goldfrank L.R. (ed).; MacGraw-Hill; Ch.84, p.1283
Heyder J., Gebhart J, Roth C., Ferron G.; 2004. Transport and deposition of hydrophilic drug particles in the lungs. In: Gradon L., Marijnissen, J.C. 2004. Optimization of Aerosol Drug Delivery (eds.). Springer Verlag, Heidelberg – FRG. pp. 139-147.
Hofmann W; Koblinger L; 1990b. Monte Carlo modeling of aerosol deposition in human lungs. Part II: Deposition fractions and their sensitivity to parameter variations. Journal of Aerosol Science. Vol. 21, no. 5, pp. 675-688. 1990.
Khan M. I. G., 2006. Encyclopedia of Heart Diseases. Academic Press; Ch.55, Effects of Smoking in Heart disease, p. 335.
Koblinger L; Hofmann W; 1990a. Monte Carlo modeling of aerosol deposition in human lungs. Part I: Simulation of particle transport in a stochastic lungs structure. Journal of Aerosol Science. Vol. 21, no. 5, pp. 661-674.
Levine R. R., Walsh C. T., Schwartz-Bloom R. D., 2000. Pharmacology: Drug Actions and Reactions, 6th ed. Taylor & Francis Group
Multz D., 2007. Personal communication by Prof. Dr.Dr.D.Mulz at the Selsonic's Workshop on the 22nd / 23rd Feb. 2007 held in Ampfing, FRG
Robinson R. J., Yu C. P., 2001. Deposition of Cigarette Smoke Particles in the Human Respiratory Tract. Aerosol Science and Technology 34: 202–215.
Yeh HC, Schum GM. 1980. Models of human lung airways and their application to inhaled particle deposition. Bull Math Biol ; 42, pp. 461-480.